

MOL # 1743

The low potency, voltage-dependent HERG blocker propafenone – molecular determinants and drug trapping

**Harry J. Witchel, Christopher E. Dempsey, Richard B. Sessions, Matthew Perry, James
T. Milnes, Jules C. Hancox, John S. Mitcheson**

Cardiovascular Research Laboratories

Department of Physiology

(HJW, JTM, JCH)

And

Molecular Recognition Centre

Department of Biochemistry

(CED, RBS)

School of Medical Sciences

University of Bristol

Bristol, BS8 1TD

UK

And

Department of Cell Physiology & Pharmacology

Medical Sciences Building

Leicester University

Leicester LE1 9HN

UK

(MP, JSM)

MOL # 1743

Running title: HERG Propafenone Molecular Determinants

† Author for correspondence:
Cardiovascular Research Laboratories
Department of Physiology
School of Medical Sciences
University of Bristol
Bristol, BS8 1TD
UK
Tel: UK +44 117 928 7817
Fax: UK +44 117 928 8923
Email: harry.witchel@bristol.ac.uk

Item	# of item (or # of words)
Text pages	23
Tables	2
Figures	9
References	30
Abstract (# words)	247 words
Introduction (# words)	500 words
Discussion (# words)	1489 words

Abbreviations: I_{Kr} , the 'rapid' delayed rectifier potassium current; MES, morpholino ethanesulphonic acid; SEM, standard error of the mean

MOL # 1743

Abstract

The molecular determinants of high-affinity HERG potassium channel blockade by methanesulfonanilides include two aromatic residues (F656 and Y652) on the inner helices (S6) and residues on the pore helices that face into the inner cavity, but determinants for lower-affinity HERG-blockers may be different. In this study, alanine-substituted HERG channel mutants of inner cavity residues were expressed in *Xenopus* oocytes, and were used to characterise the HERG channel binding-site of the antiarrhythmic propafenone. Propafenone's blockade of HERG was strongly dependent on residue F656, but was insensitive or weakly sensitive to mutation of Y652, T623, S624, V625, G648, or V659, nor did it require functional inactivation. Homology models of HERG based on KcsA and MthK crystal structures, representing the closed and open forms of the channel, respectively, suggest propafenone is trapped in the inner cavity and is unable to interact exclusively with F656 in the closed state (whereas exclusive interactions between propafenone and F656 are found in the open-channel model). These findings are supported by very slow recovery of wild-type HERG channels from block at -120 mV, but extremely rapid recovery of D540K channels that re-open at this potential. The experiments and modelling suggest the open-state propafenone binding-site may be formed by the F656 residues alone. The binding-site for propafenone (which may involve pi-stacking interactions with two or more F656 side-chains) is either perturbed or becomes less accessible due to closed-channel gating. This adds further evidence for the existence of gating-induced changes in the spatial location of F656 side-chains.

MOL # 1743

Introduction

Pharmacological blockade of the cardiac ‘rapid’ delayed rectifier potassium (K^+) current (I_{Kr}) is commonly associated with a drug’s propensity to cause acquired long QT syndrome (Roden *et al.*, 1996). The alpha sub-unit of the I_{Kr} channel is encoded by *HERG* (Sanguinetti *et al.*, 1995). Molecular determinants of this channel’s blockade by the archetypal high potency HERG-blockers, the methanesulfonanilides, reside in the inner cavity of the channel pore, being comprised of amino acid residues in the H5 loop (adjacent to the selectivity filter) and the S6 transmembrane domain (Mitcheson *et al.*, 2000a; Lees-Miller *et al.*, 2000). For all drugs tested, the molecular determinants include the amino acid residues F656 and Y652 (with the exceptions of vesnarinone, which does not require Y652 (Kamiya *et al.*, 2001), and fluvoxamine, which can block HERG when F656 or Y652 are mutated (Milnes *et al.*, 2003)), and in many cases the molecular determinants additionally include a combination of T623, S624, V625, G648, and V659. Most drugs with a high-affinity for HERG, have been shown to have an open-state-dependent blockade mechanism (Spector *et al.*, 1996). Open-state blockade of HERG may involve drug trapping (e.g. MK-499 (Mitcheson *et al.*, 2000b)), a ‘foot in the door’ type mechanism (e.g. chloroquine (Sanchez-Chapula *et al.*, 2002)), or rapid unbinding upon repolarisation (e.g. vesnarinone (Kamiya *et al.*, 2001)); these different mechanisms can often be differentiated by the kinetics of current decay during deactivation.

The Class Ic antiarrhythmic drug propafenone (Funk-Brentano *et al.*, 1990) can cause QT prolongation and pro-arrhythmia (Rehnqvist *et al.*, 1984; Hii *et al.*, 1991). We and others have previously shown that propafenone blocks native I_{Kr} and HERG with an open-state-dependent mechanism (Duan *et al.*, 1993; Delpon *et al.*, 1995; Mergenthaler *et al.*, 2001; Paul *et al.*, 2002), although at a substantially lower potency than methanesulfonanilides block HERG. The goal of this study was to determine how open-state-dependent blockade occurred with this drug; in particular, whether the low-affinity blockade by propafenone

MOL # 1743

shared mechanistic traits of the high-affinity blockade by methanesulfonanilides at two levels: molecular determinants and drug trapping. This report demonstrates that the voltage-dependent, low-affinity blockade of HERG by propafenone deviates from that previously described for chloroquine (Sanchez-Chapula *et al.*, 2002), and the molecular mechanism also differs from previous observations for high-affinity blockers. This finding led to the question of whether existing structural models of HERG channel blockade were sufficient to describe the block by propafenone. Consequently, an *in silico* model of HERG channel blockade in the open-state was then developed, and docking simulations were performed. Comparison of the results from the computer simulations using our new open-channel model with those using a closed-channel model lead us to propose an alternative open-channel blocking mechanism. This mechanism incorporates drug trapping in the closed state and strong interactions with F656 in the open-state of the channel.

MOL # 1743

Materials and Methods

Measurements of heterologous HERG currents

Isolation of *Xenopus* oocytes, their handling and injection with mRNA, creation of mutant channel cDNAs, and two electrode voltage clamp with rapid solution switching was performed as described previously (Mitcheson *et al.*, 2000a; Mitcheson *et al.*, 2000b). Capped RNA from linear template DNA was made using the mMessage mMachine kit, and between 5 and 30 ng of RNA was injected into each oocyte and allowed to express between 1 and 4 days before making recordings. The electrode solution was 3 M KCl. The extracellular recording solution was low in Cl⁻ (which was substituted for by MES — morpholino ethanesulphonic acid) and consisted of (in mM): 96 NaMES, 2 KMES, 2 CaMES₂, 5 HEPES, 1 MgCl₂, adjusted to pH 7.6 with methane sulphonic acid (Mitcheson *et al.*, 2000a; Mitcheson *et al.*, 2000b). Substitution of chloride by MES results in substantially reduced endogenous chloride currents (see Figure 5 in (Mergenthaler *et al.*, 2001)). Some mutants (e.g. T623A and G648A) have a leftward shifted voltage dependence of inactivation and do not conduct current under standard recording conditions. These mutants were investigated using a “high K⁺” extracellular superfusate containing 96 mM K⁺ and 2 mM Na⁺ (Sodium). Propafenone (Sigma) was dissolved directly in extracellular recording solutions by heating briefly to 70°C.

The voltage command protocols (applied at room temperature) used for determining molecular determinants of blockade were: all cells held at -90 mV, then a 2 second step to 0 mV, followed by observation of tails for 2 seconds at -70 mV for wild-type HERG and most mutants (interpulse interval 10 seconds). For F656A and V659A tail currents were observed at -140 mV, and V625A tail currents were observed at -90 mV. For most experiments the response to propafenone was quantified from measurements of peak tail current amplitude.

MOL # 1743

S631A and G628C/S631C block were quantified from isochronal ‘end pulse’ currents, which were larger than the tail currents (comparisons of results derived from S631A tail currents and S631A end pulse currents were very similar — G628C/S631C tail currents were too small to measure).

Steady-state HERG current baselines were attained by repetitively pulsing to 0 mV (100-200 sweeps). A constant flow of superfusate was applied with a ‘rapid solution switcher’ (adapted for oocytes from (Levi *et al.*, 1996)). Initial application of propafenone always began with exposure to the drug for two minutes while maintaining the holding potential of the oocytes at –90 mV. Initial blockade invariably occurred in less than 200 ms during the first sweep at 0 mV; this type of blockade we have called “pseudo-steady-state” because block increased very slowly thereafter. Recovery from pseudo-steady-state block did not occur in closed-channels but could be induced after washing out the bath with control solution for 5 minutes and opening channels by a prolonged depolarisation. Steady-state drug blockade resulted from more prolonged exposure to propafenone accompanied by extensive pulsing (>75 sweeps), and the potency of steady state blockade was slightly greater than that of pseudo-steady-state blockade. Steady-state block was only slightly reversible. The difference between steady-state and pseudo-steady-state block may possibly involve drug accumulation intracellularly and binding associated with the lipophilic yolk sac of the oocyte. All the experiments on the molecular determinants of blockade were performed using steady-state block; experiments on drug trapping were done using pseudo-steady-state block. IC_{50} values for propafenone were determined by fitting the concentration response data with the Hill function $Y=1/[1+10^{((\text{Log}IC_{50}-X)*n_{\text{Hill}})]}$ (GraphPad Prism, GraphPad Software Inc., San Diego, CA, USA), where X is the logarithm of concentration and Y is the blockade; maximum and minimum values for the blockade were fixed at 1 and 0 at points 3 orders of magnitude from the observed maxima and minima. Values for IC_{50} ’s were calculated with

MOL # 1743

95% confidence intervals (CI); all other statistical measures are presented as mean \pm standard error of the mean (SEM).

Computer modelling

HERG pore homology models were constructed based on sequence homology with the pore regions of KcsA (closed-pore model) and MthK (open-pore model) and using as templates the X ray crystal structures determined by Mackinnon and co-workers (Doyle *et al.*, 1998; Jiang *et al.*, 2002) (PDB accession codes: KcsA: 1BL8, MthK : 1LNQ). Only the sequence corresponding to the selectivity filter, pore-helix and S6 helix were modelled since this region provides all the residues that comprise the pore, and because the homologies of S5 of HERG with the outer TM helices of KcsA and MthK are not fully defined.

Homology models were constructed within the Biopolymer and Builder modules of InsightII (Accelrys) by “mutating” the amino acids of KcsA or MthK to the corresponding amino acids of HERG. For the closed-pore model, side-chain rotamers were chosen to match the rotamers of KcsA up to the side-chain β atoms, where relevant. Since the MthK crystal structure contains backbone coordinates only, the side-chain rotamers were introduced according to the most highly populated rotamer in the crystal structure database for the relevant secondary structure type. Each model was visually inspected and severe spatial clashes of amino acid side-chains were relieved by selecting the side-chain rotamer that gave the lowest energy. Finally each model was energy minimised by 2000 steps of steepest descents using Discover. The structures of both stereoisomers of propafenone were constructed within InsightII and energy minimised. Since the tertiary amino group has a pK_a of 8.8, this amino group was maintained in its protonated (charged) form. The two stereoisomers of MK-499 [(+)-*N*-[1'-(6-cyano-1, 2, 3, 4-tetrahydro-2(*R*)-naphthalenyl)-3,4-dihydro-4(*R*)-hydroxyspiro(2H-1-benzopyran-2,4'-piperidin)-6-yl]methanesulfonamide] were also constructed (positively charged secondary amino group) for docking runs for

MOL # 1743

comparison with structures previously produced (Mitcheson *et al.*, 2000a). This provides a check on the extent to which separate docking algorithms and different homology models produce a coherent picture for docking of this drug into the closed-pore HERG model. We found that the lowest energy structures of MK-499 bound to our closed-channel homology model were generally similar to that described previously (Mitcheson *et al.*, 2000a) for binding of MK-499 to a KcsA-based closed-channel homology model using FLOG (Flexible Ligands Oriented on Grid) docking methods (not shown).

Docking runs were performed using FlexiDock within Sybyl 6.9. FlexiDock uses a genetic algorithm to explore the conformational and orientational space that defines possible interactions between the ligand and its binding-site. The program requires initial placement of the ligand into a potential binding-site, the latter being defined as the amino acids selected together with any atoms within 4.5 Å. FlexiDock allows selected bonds in both the ligand and binding-site to be rotated during sampling of conformational space. Based on the mutagenesis data, the binding-site for propafenone is within the pore, and incorporates interactions with F656. However, in order not to bias the modelling, the binding-site in most runs included most of the amino acid side-chains on the S6 helix that project into the pore in closed state models. These are G648, S649, Y652, F656 and S660. In some runs the residues facing the inner cavity of the pore below the selectivity filter (T623, S624, and V625) were also included. All possible rotatable bonds within the ligands were selected, and all rotatable bonds in the side-chains that define the potential binding-site were selected (excluding trivial bond rotations involving X-H bonds).

For the propafenone-HERG models presented here at least 20 FlexiDock runs were made with different starting positions and orientations of the ligand within either the open or closed-state models. Normally, runs with 20,000 generations within the genetic algorithm were made to obtain a series of 6-12 different low energy structures. These were used as

MOL # 1743

starting points for longer (80,000-120,000 generation) runs which normally gave high levels of convergence (70-80%) indicating that the lowest energy structure within the particular set of minima explored in that run had been achieved. A total of approximately 4,000,000 FlexiDock generations were sampled for propafenone binding to each of the open and closed-channel models (table 1).

MOL # 1743

Results

S6 inner helix mutations and their effects on propafenone mediated blockade

In order to determine whether the molecular determinants of blockade of HERG by propafenone were similar to those previously described in the S6 inner helix, as observed with other drugs (Mitcheson *et al.*, 2000a), channels having mutations of residues modelled to line the inner cavity and selectivity filter were tested for functional drug blockade; the testing of these mutants does not exclude the possibility that additional binding interactions might occur for S5 residues and other S6 residues thought not to line the pore (Gessner *et al.*, 2004; Ishii *et al.*, 2001).

A propafenone concentration (50 μM) causing profound blockade of wild-type HERG current (I_{HERG}) was used to test HERG channel mutants (Figure 1). It inhibited wild-type I_{HERG} tails at -70 mV by $96.4 \pm 0.1\%$ (mean \pm SEM, 2 mM $[\text{K}^+]_o$; N = 5), and at -140 mV by $79.6 \pm 4.9\%$ (2 mM $[\text{K}^+]_o$; N = 5). With raised $[\text{K}^+]_o$ (96 mM), wild-type I_{HERG} tails at -70 mV were inhibited by $88.3 \pm 2.5\%$ (N = 5). 50 μM propafenone blocked the mutant HERG channel F656A by only $5.0 \pm 9.7\%$ (N = 5), demonstrating that, as for the methanesulfonanilides, dofetilide and MK-499 (Lees-Miller *et al.*, 2000; Mitcheson *et al.*, 2000a), the F656 residue is a critical determinant of HERG channel blockade for propafenone. To estimate the order of magnitude of attenuation, we also tested 100 μM and 300 μM propafenone, which blocked F656A by $22.6 \pm 8.8\%$ and $66.4\% \pm 2.6\%$, respectively (N = 5); higher concentrations of propafenone were difficult to solubilise, but fitting the three concentrations tested to a Hill plot led to an estimate of an $\text{IC}_{50} \sim 100$ -fold higher than wild-type HERG (table 2). This shift is similar to values seen with F656A for cisapride and terfenadine (Mitcheson *et al.*, 2000a). F656 has also been shown to be a molecular determinant for the other class I antiarrhythmic tested, quinidine (Lees-Miller *et al.*, 2000);

MOL # 1743

quinidine blocks wild-type HERG at a similar potency to propafenone when measured under similar conditions (Paul *et al.*, 2002).

In contrast, for all other mutations tested (located in either the pore helix or S6 regions, and selected on the basis of being molecular determinants for those agents previously studied (Mitcheson *et al.*, 2000a; Kamiya *et al.*, 2001; Sanchez-Chapula *et al.*, 2002)) 50 μ M propafenone blocked the other channels' tail currents much more than those of F656A (see Figure 1). G628C/S631C (a double mutant that does not inactivate) was blocked by $85.9 \pm 2.2\%$ ($N = 5$), showing that inactivation is not obligatory for block by propafenone. The finding that propafenone block was only slightly altered by mutation of Y652 was particularly unexpected, since this residue also faces into the inner cavity of the channel, is located next to F656 (separated by one turn of the S6 α -helix) and has been shown to be critical for binding to nearly all other compounds investigated. Vesnarinone, the only other low-affinity blocker investigated in detail (Kamiya *et al.*, 2001), also did not show a strong interaction with Y652, and Kamiya *et al.* suggested that the reduced blockade potency of vesnarinone might be due to the lack of a strong Y652 interaction combined with the lack of drug trapping (due to vesnarinone being uncharged). Propafenone is charged and does exhibit drug trapping, but it lacks the Y652 interaction as does vesnarinone; this is concordant with its functional HERG blockade potency in *Xenopus* oocytes, as propafenone falls between vesnarinone and the high-affinity blocking methanesulfonanilides. Overall, the features of propafenone blockade of HERG differ from those of vesnarinone which was shown to have wide spectrum of molecular determinants in this region, including strong interactions with the residues at the base of the pore helix (T623, S624, V625). Whilst the testing of the mutants selected does not exclude the possibility that additional binding interactions might occur between S5 residues or other S6 residues thought not to line the

MOL # 1743

pore, our data reveal a distinct profile for propafenone in respect of those residues thus far considered to be important for drug-HERG interactions.

Drug trapping of propafenone

Experimental evidence suggested that drug trapping of propafenone by HERG occurred. First, unlike many other low-affinity HERG-blockers (e.g. vesnarinone (Kamiya *et al.*, 2001) and chloroquine (Sanchez-Chapula *et al.*, 2002)), recovery from propafenone-mediated block did not occur while holding V_m at -90 mV (not shown). However, unblock did occur if the drug was washed off for several minutes *and* channels were subsequently opened by depolarisation (Figure 2). Thus, access to and escape from the inner cavity is dependent on opening of the activation gate. Second, there were no significant changes in any deactivation time constants when comparing currents in control and $3 \mu\text{M}$ propafenone containing solutions ($P > 0.30$ for t tests during deactivation at -140 , -120 and -70 mV following a steady state level of activation induced by a five second step to 0 mV). Rapid recovery from block or unblock that results from channel deactivation often leads to a slowing of the current decay during channel deactivation (i.e. an apparent increase in deactivation time constant) because the activation gate is unable to close while drug is bound to the channel. This data suggests that propafenone does not exhibit a foot in the door block of HERG.

To determine whether or not propafenone becomes trapped within the inner cavity by closure of the activation gate, we used the D540K mutant of HERG, which can open upon hyperpolarisation as well as upon depolarisation (Sanguinetti and Xu, 1999). At the single channel level the mechanism of D540K's increased conductance is not associated with any change in single channel conductance (Mitcheson *et al.*, 2000b) and is due to destabilisation of the closed state. This mutant channel allowed us to test whether having the channel in a conducting state whilst strongly directing the driving force for both K^+ ions and positively-charged propafenone toward the cytosol was sufficient to relieve channel blockade. With

MOL # 1743

D540K channels, repeated hyperpolarising voltage commands led to channel opening and the diminution of the channel block in the presence of the methanesulfonamide MK-499 (Mitcheson *et al.*, 2000b), suggesting that the mechanism of the open-channel block was based on trapping of the drug inside the channel inner cavity during channel closure.

D540K-HERG was blocked by 3 μ M propafenone when depolarising pulses were applied. Rapid recovery from block (within 200 ms) could occur during a single hyperpolarising pulse to -120 mV, even in the continued presence of drug. Such recovery did not occur with repolarisation back to -70 or -40 mV (Figure 3). The observation that hyperpolarisation-dependent channel opening was critical for recovery was underscored by the fact that no recovery from block occurred with the D540A mutant, which (like wild-type HERG) does not open with hyperpolarisation. All these data support the idea that the mechanism of propafenone blockade of HERG involves drug trapping, with rapid on and off rates, and that after initial opening and commencement of blockade, propafenone can and probably does reside inside the inner cavity in the closed state; however, we cannot rule out that propafenone may interfere with channel closure, resulting in a configuration in which the propafenone-HERG inner cavity configuration is neither open nor closed (e.g. partially closed) while being functionally blocked. We propose that in the open-hyperpolarised state the blockade of the channel by propafenone was compromised, perhaps because the F656 binding-site (which may consist of side-chains from more than one of the four F656 residues) is perturbed or inaccessible in this state.

To determine whether or not hyperpolarisation *per se* (i.e. without maintaining a highly conducting state) was sufficient to relieve channel blockade, blockade was determined for fully activated wild-type HERG after increasing durations of deactivation at -120 mV (see Figure 4). The effect of hyperpolarisation on recovery from block of wild-type HERG was assessed by stepping back to 0 mV and measuring the instantaneous component of current

MOL # 1743

resulting from the increase in K^+ ion driving force at this potential. Currents were curve fitted and extrapolated back to the beginning of the voltage step to give a measure of current availability.

In contrast to D540K-HERG, blockade of wild-type HERG by propafenone was not relieved at -120 mV between 20-120 ms (after 120 ms currents were too small to compare), nor was block relieved in similar protocols when deactivation took place at -40 mV or -70 mV (Figure 4). The lack of time-dependent recovery from blockade during deactivation is consistent with the hypothesis that propafenone was trapped in wild-type HERG; however, the lack of recovery between 20-120 ms suggests that there is a difference in the propafenone binding-site in the deactivating wild-type channel versus the OH state in the D540K channel. The differences in percentage block at -120 compared with -70 or -40 mV are relatively small, occur within the first 10 ms and may in part be due to differences in ionic flux through the pore. Although the wild-type channel does not release propafenone upon repolarisation, the results for wild-type HERG and D540K suggest that channel opening is necessary (although not sufficient in the case of wild-type) for the drug to exit the channel. Thus, the mode of open-state blockade (as previously described (Duan *et al.*, 1993; Mergenthaler *et al.*, 2001; Paul *et al.*, 2002)) involves drug trapping or another mechanism that holds the drug within the channel when the channel is closed.

Mutant channels do not release propafenone faster than wild-type when closed

The lack of reversible blockade while the channel is closed could be due to drug trapping *per se* or result from closed-state interactions with inner cavity residues. Such interactions would be difficult to measure directly using electrophysiological techniques since the channels are in a non-conducting state. However, monitoring recovery from block following drug washout provides an indirect means of looking at drug binding affinity since experimental interventions that lower binding affinity would speed up the kinetics of

MOL # 1743

recovery from block and un-trapping. Therefore, we compared wild-type channel recovery from block after drug washout at negative potentials with the same measurements from inner cavity mutants. To test the amount of blockade, while minimising the time spent in the open-state (thus optimising the electrophysiological measurement of blockade of the closed-channel), a short depolarising pulse (a 40 ms step to +40 mV) was used to quickly open the channels followed by a short repolarising step (200 ms to -60 mV) to allow for the observation of the comparatively larger tail currents (the “sampling protocol,” see Figure 5). Measurements of fractional blockade (normalised to the first sweep of the protocol) were made at a baseline in control solution (last sweep of the protocol before adding drug), in pseudo-steady-state blockade by 10 μ M propafenone, and then in the first sweep after washout of the drug for five minutes — washout was performed while the holding potential was maintained at -120 mV to maintain channel closure. An identical series of experiments was then performed on the same oocyte but with only a thirty second washout. The measured currents for each oocyte were nearly identical for the experiments involving the five minute vs. the thirty second washout (Figure 5C). If two variables are identical, then a regression of one on the other should result in a zero intercept and a slope of unity. A linear regression of fractional blockade values for the “five minute” washout data on those for the “thirty second” washout data (e.g. the sweeps in Figure 5Ai on 5B) had a slope that was not significantly different from 1 (0.9949, 95% confidence interval = 0.9236 to 1.0663, $P = 0.872$) and had a y-intercept was not significantly different from 0 (0.0038, 95% confidence interval = -0.0187 to 0.0263, $P = 0.701$, and for the entire model: $R^2 = 0.9936$). This result suggests that the recovery from blockade is effectively independent of the time spent in the closed state when compared with the level of recovery from blockade that occurs in only 40 ms in the open-state. This rapid recovery from blockade during an initial opening of the channel can be seen in Figures 5A and 5B in the washout sweeps, which show an increasing tail current (rather

MOL # 1743

than a tail current peak) that is reminiscent of the cross-over currents associated with a “foot in the door” type of blockade; this cross-over current is only observed with propafenone immediately after the drug has been washed out (and the drug’s concentration gradient would be out of the channel), whereas true “foot in the door” blockade current cross-over occurs with the drug present in the superfusate. Thus, recovery from blockade after washout of propafenone is very rapid when the wild-type channels are open (> 50% recovery in less than 10 ms) and is virtually undetectable in the time scale tested (five minutes) when the channels are held closed.

Even though recovery from propafenone blockade of the wild-type channel is extremely slow when the channel is in the closed state, it is possible to test whether the mutations tested (particularly F656A) cause a change in the level of recovery from blockade when the channel is held in the closed state (-120 mV). This was done for a selection of mutant HERG channels in a manner similar to that shown in Figure 5Ai, in which the mutant channels were exposed to a level of propafenone that would elicit a fractional block of ~ 50%, and then the propafenone was washed off for five minutes (Figure 5D); the varying concentrations of propafenone are necessary to establish comparable initial levels of blockade, and is useful because recovery from blockade after the drug-containing superfusate has been replaced by control solution should depend on the level of blockade but be independent of the previous concentration of drug. Recovery from propafenone block of Y652, V625A and S624A was similar to or slower than WT HERG. Only F656A showed a quickening of recovery from block, although it was not significantly different from wild-type ($P > 0.05$). One way analysis of variance (ANOVA) with post hoc Bonferroni multiple comparison tests showed that the percent recovery after five minutes of washout for the various mutant channels was different after similar levels of blockade by propafenone ($P = 0.0002$). This difference was individually statistically significant for wild-type vs. S624A, Y652A vs. S624A, F656A vs.

MOL # 1743

S624A, and F656A vs. V625A ($P < 0.01$ for all). S624A has the unanticipated reverse effect on the wild-type channel of slowing the reversibility of blockade. This same mutation leads to an increased reversibility of blockade by the chlorobenzene derivative clofilium, presumably due to the interaction of the halogen of clofilium with this region of the HERG structure (Perry *et al.*, 2004); an analogous halogen is absent from propafenone. These experiments suggest that none of the mutations tested significantly reduces propafenone's interaction with the channel in the closed state, although it does not exclude the possibility that F656A may have a small effect in that way.

Voltage-dependent mechanism of blockade predicted from homology models

The mechanism of HERG blockade by propafenone has been previously demonstrated to be voltage-dependent (Arias *et al.*, 2003; Paul *et al.*, 2002; Mergenthaler *et al.*, 2001). Given that our data suggests that propafenone can interact with the residues of the inner cavity (as predicted by previous models based on the KcsA closed-channel structure), but primarily only at F656, it is possible that the voltage-dependence may be due to gating-dependent effects on accessibility or spatial positioning of the F656 side-chains for drug interactions. To test the latter possibility, we studied docking of propafenone into closed- and open-state homology models of the HERG pore region using the crystal structure co-ordinates of KcsA (closed-channel) and MthK (open-channel) as templates (Doyle *et al.*, 1998; Jiang *et al.*, 2002). The homologies are shown in Figure 6, and the resulting models are shown in Figures 7A and 7B. Analysis of docking interactions with homology models cannot give unequivocal answers about the nature of the drug binding. Nevertheless, multiple FlexiDock runs of MK-499 in the closed-channel model resulted in a relatively small set of low energy structures in which the drug adopted a reproducible conformation (not shown) and made a well-defined set of interactions with HERG residues facing the channel inner cavity (similar to those found by Mitcheson *et al.*, 2000a)). This differed for propafenone, in which FlexiDock located a large

MOL # 1743

variety of different low energy structures for the interaction with either open or closed-channel models, although these were found to cluster in terms of their dominant interactions.

Inspection of docking to open and closed-channel homology models suggests that the mutagenesis data for propafenone-mediated blockade may be best rationalised by interactions with the open-channel model. The “splaying out” of the terminal regions of the pore-lining helices in the open-channel model (Figure 7B) renders the F656 side-chains highly accessible to molecules approaching the channel from the cytoplasmic side of the membrane (the C α – C α separation across the pore at the level of F656 in the open-channel model is around 20 Å). A significant preference for interactions involving F656 over Y652 was observed in docking of propafenone to the open-channel model. Both aromatic rings of propafenone can make simultaneous π -stacking interactions with aromatic rings of F656 on adjacent, or opposite, channel sub-units. Using a variety of initial conditions, FlexiDock was able to find several different low energy conformations, and almost all of the lowest energy structures of propafenone involved simultaneous π -stacking interactions of propafenone’s aromatic rings with adjacent aromatic rings of two F656 residues (the lowest energy structure is shown in Figures 7B and 7D).

As with the open-channel model, the interactions of propafenone with HERG residues in the inner cavity of the closed-channel model were promiscuous, and a variety of different low energy conformations and interactions were found. Nevertheless, in all starting positions and configurations of both stereoisomers of propafenone in the closed-channel model, the lowest energy binding interactions were achieved only on movement of the drug into the inner cavity below the selectivity filter (the lowest energy structure is shown in Figures 7A and 7C). Furthermore, in the closed-channel model the channel is constricted in the region of F656 (C α – C α distance across the pore is 10 Å), and there is simply not enough space for

MOL # 1743

propafenone to make simultaneous π -stacking interactions with F656 side-chains involving both of propafenone's aromatic rings (see Figures 7E and 7F).

A summary of all the FlexiDock runs, for both open- and closed-channel models, is shown in Figure 8. In open-state models a cluster of low energy docking structures were obtained in which near- or fully-exclusive interactions between propafenone and F656 side-chains were obtained. In closed state models, no low energy structures were obtained having exclusive propafenone-F656 $\pi:\pi$ interactions. In most low energy structures from the closed-channel model, mixed interactions of propafenone with both F656 and Y652 aromatic rings were found. These generally corresponded to the migration of propafenone into the inner cavity below the selectivity filter. A number of runs in which propafenone was constrained to interact with the closed model at the level of the F656 residues resulted in very poor energies (these correspond to the grouping of runs with high propafenone-F656 and zero or near-zero propafenone-Y652 interactions). Thus, only in open-channel models were exclusive interactions with F656 (rather than Y652) side-chains reproducibly found. The conformational lability of propafenone, and its ability to make a range of different interactions with F656 residues in the modelling by FlexiDock, may be a reflection of the low-affinity of the drug with HERG. The failure of modelling the closed-channel's interaction with propafenone to provide a consistent low energy conformation that was concordant with the observed mutagenesis data may indicate that the interactions between propafenone and the closed-channel are weaker than the interactions with the open-channel. Furthermore, it suggests that the main blocking criterion in the closed-channel may be spatial restriction due to the ring of the four F656 side-chains (which are closer together in the closed state model compared to the open-state model) that prevents egress of the propafenone molecule from the channel's inner cavity. This further supports the proposition that the voltage-dependent blocking mechanism includes drug trapping.

MOL # 1743

Discussion

This study demonstrates that of the inner cavity residues known to be molecular determinants of pharmacological blockade of HERG, F656 is the most important one for propafenone blockade. We propose that the binding of propafenone to HERG is defined by interactions with an open-channel state (inactivation is not required) in which the F656 side-chains are accessible and form the principal binding-site. On channel closure the drug is held or trapped in the inner cavity. Because there is no time-dependent recovery from blockade in the wild-type channel during current deactivation, rapid reversibility of blockade with the next depolarization may depend upon events occurring after closure of the channel. One possible sequence of events consistent with our results would be 1) channel closure and drug trapping accompanied by 2) release of the drug from F656-binding-site into the inner cavity, followed by 3) drug release from the inner cavity after subsequent re-activation.

The structural models predicted that spatial restrictions near F656 could not maintain propafenone in the F656-bound (and presumably blocking) conformation in a KcsA-based closed-channel model, and that these spatial restrictions were responsible for trapping the drug in the inner cavity of the channel during long closures. In closed-channel homology models the pore is constricted at the level of the F656 residues ($C\alpha$ - $C\alpha$ separation across the pore is 10 Å), and there is insufficient space to accommodate propafenone in configurations that allow exclusive interactions only with F656 side-chains. While there is ample room in the inner cavity for trapping of propafenone, all low energy binding modes involved significant interactions with Y652 (Figures 7A, 7C). Thus, agreement between the mutagenesis and docking data was only obtained in the open-state model where nearly exclusive interactions of propafenone with F656 were obtained (Figure 8). Presumably the Y652:propafenone interactions in the closed-channel model are not as energetically favourable as F656:propafenone interactions once the channel has opened. These results

MOL # 1743

indicate a real and significant difference between HERG's interaction with propafenone versus its interactions with high-affinity blockers like MK-499; indeed we found low energy docking modes of MK-499 with the closed-channel model that were both fully consistent with mutagenesis data, and very similar to those previously obtained in an independent computational docking analysis (Mitcheson *et al.*, 2000a).

While the data presented here support propafenone's interaction with the open-state and do not support strong interaction with the closed state, the situation regarding the inactivated state(s) also warrants consideration. One study of propafenone's block of wild-type HERG (Arias *et al.*, 2003) concluded that HERG might have a higher affinity for propafenone in the inactivated (rather than the open) channel state. However, in the present study two non-inactivating mutants (S631A and S628C/S631C) were effectively blocked by propafenone, indicating that channel inactivation is not obligatory for blockade to occur (*cf.* class Ia antiarrhythmic HERG-blockers disopyramide (Paul *et al.*, 2001), quinidine (Lees-Miller *et al.*, 2000) and procainamide (Ridley *et al.*, 2003)). This does not exclude some affinity of HERG for propafenone in the inactivated state, so long as the affinity in the inactivated state is quantitatively similar in level to the open-state affinity.

Mergenthaler *et al.* (2001) suggested that propafenone acts on HERG from the cytoplasmic side of the membrane and binds to a site part way across the transmembrane electric field. They found that block was substantially reduced by lowering the pH of the extracellular solution to 6. Propafenone's pK_a is 8.8, suggesting that at pH 7.4 it is ~96% protonated, and at pH 6, it is ~99.8% protonated; thus at acid pH it would be predicted that propafenone would be less able to gain access to the cytosolic surface of the channel because of decreased membrane permeability. They also found that block increased continuously at progressively depolarised potentials (even at potentials above which the increase in open probability was only slight) and calculated that propafenone bound to a site with a fractional

MOL # 1743

electrical distance $\delta = 0.2$ across the electric field. Other Woodhull analyses have also been performed that collectively suggest that propafenone senses between 9 and 27 % of the transmembrane field measured from the interior (Mergenthaler *et al.*, 2001; Arias *et al.*, 2003; Paul *et al.*, 2002). Thus, the drug's binding-site is part way across the transmembrane electrical field, nearer to the cytoplasmic side of membrane. This is consistent with the fact that F656 is presumed to be located toward the cytoplasmic end of the pore inner cavity and that F656A was the only one of the mutants tested in which blockade by 50 μM propafenone was dramatically attenuated.

The mechanism of recovery from block by propafenone is probably not due to a voltage dependent process such as 'knock off' by K^+ influx at hyperpolarised potentials, since high extracellular K^+ had only a small change on IC_{50} and recovery from block. Blockade of the wild-type channel during repolarisation/deactivation was not time dependent (at least not within the range of 20-120 ms) but showed some voltage dependence (Figure 4); this suggests that recovery from block was unlikely to be due to voltage dependence of channel deactivation, but rather resulted from an action of the electric field on drug binding. Thus, our data are concordant with the notion that the electric field may act directly on the drug molecule and can drive propafenone out of the channel inner cavity (i.e. towards the cytoplasm) so long as the channel is open when the membrane is hyperpolarised.

The potency of propafenone's blockade of HERG

Based on previous studies of the molecular determinants of HERG pharmacology, we and others have postulated that π -stacking between aromatic groups of the drug and F656 and Y652 of HERG are important for high-affinity binding (Mitcheson *et al.*, 2000a; Lees-Miller *et al.*, 2000). Fernandez *et al.* (Fernandez *et al.*, 2004) have recently demonstrated that the potency for block by MK-449, cisapride and terfenadine was well correlated with measures of hydrophobicity at position 656, especially the 2-D approximation of the van der Waals

MOL # 1743

hydrophobic surface area of the side-chain of the residue. For residue 652, an aromatic side group was essential for high-affinity block, suggesting the importance of a cation- π interaction between Y652 and the basic tertiary nitrogen of these drugs. Concordant with this, propafenone only weakly interacts with Y652, and its potency for blockade is also found to be lower than methanesulfonanilides. Pharmacophore models predict that important features of potent HERG channel blockers are 1) a basic nitrogen that is usually protonated at physiological pH, and 2) three hydrophobic centers of mass (centroids) arranged in a specific spatial pattern around the centrally located nitrogen (Cavalli *et al.*, 2002; Ekins *et al.*, 2002). For many potent HERG-blockers, these centroids are aromatic groups. Propafenone does not have this many aromatic groups, the nitrogen is not centrally located, and the arrangement of these groups is more flexible than in high-affinity HERG-blockers such as MK-499 (see Figure 9).

We found that the IC_{50} for propafenone's blockade of heterologous HERG expressed in *Xenopus* oocytes was 2.16 μ M (Table 2), which is 5-fold larger than the IC_{50} we have previously observed in mammalian cells expressing HERG (Paul *et al.*, 2002); the greater potency of drug block in mammalian cells compared with oocytes is a common finding and may be related to the lipophilic yolk sac in oocytes that acts to sequester the drug. Our IC_{50} of 2.16 μ M is 7-fold lower than the potency determined by Mergenthaler *et al.* (2001), who also used *Xenopus* oocytes. The reason for the difference in IC_{50} between their study and our own is not clear, but it may result from differences in recording conditions and from the reduced contamination by endogenous currents in the present study.

Conclusions

We have investigated the molecular determinants of HERG blockade by propafenone, a clinically important class Ic antiarrhythmic agent. Our results show for the first time that propafenone is retained in the channel due to gating upon repolarisation. This may have

MOL # 1743

important implications for rapid onset of I_{Kr} block during cardiac action potentials since it ensures that the drug remains close to its receptor. The mutagenesis studies suggest that, of all HERG residues previously shown to mediate drug blockade, F656 is the only residue facing into the cavity with a role in propafenone binding; however, we cannot exclude that propafenone may have additional interactions with residues in S5 or S6 that have not previously been shown to be determinants of drug blockade of HERG. Furthermore, docking simulations using computer models of both the open- and closed-channel suggest that propafenone can only make exclusive interactions with F656 in the open-state. Our results additionally support the idea that, at the molecular level, analysis of binding of HERG-blockers should consider both open- and closed-channel states, and that this may be particularly relevant for low-affinity blockers. Finally, we conclude that the accessibility of the F656 residues forming the binding-site to drugs in the inner cavity changes between the open and closed states.

MOL # 1743

Acknowledgements

We gratefully acknowledge technical support from Kate Metcalfe and Seung Ho Kang, computational support from Peter Dickens, and guidance from James Walsh and James Stelfox.

MOL # 1743

Reference List

Arias C, Gonzalez T, Moreno I, Caballero R, Delpon E, Tamargo J and Valenzuela C (2003) Effects of Propafenone and Its Main Metabolite, 5-Hydroxypropafenone, on HERG Channels. *Cardiovasc Res* **57**:660-669.

Cavalli A, Poluzzi E, De Ponti F and Recanatini M (2002) Toward a Pharmacophore for Drugs Inducing the Long QT Syndrome: Insights From a CoMFA Study of HERG K⁺ Channel Blockers. *J Med Chem* **45**:3844-3853.

Chelli R, Gervasio FL, Procacci P and Schettino V (2002) Stacking and T-Shape Competition in Aromatic-Aromatic Amino Acid Interactions. *J Am Chem Soc* **124**:6133-6143.

Delpon E, Valenzuela C, Perez O, Casis O and Tamargo J (1995) Propafenone Preferentially Blocks the Rapidly Activating Component of Delayed Rectifier K Current in Guinea Pig Ventricular Myocytes. *Circ Res* **76**:223-235.

Doyle DA, Morais Cabral JH, Pfuetzner RA, Kuo A, Gulbis JM, Cohen SL, Chait BT and Mackinnon R (1998) The Structure of the Potassium Channel: Molecular Basis of K⁺ Conduction and Selectivity. *Science* **280**:69-77.

Duan D, Fermini B and Nattel S (1993) Potassium Channel Blocking Properties of Propafenone in Rabbit Atrial Myocytes. *J Pharmacol Exp Therapeu* **264**:1113-1123.

MOL # 1743

Ekins S, Crumb WJ, Sarazan RD, Wikel JH and Wrighton SA (2002) Three-Dimensional Quantitative Structure-Activity Relationship for Inhibition of Human Ether-a-Go-Go-Related Gene Potassium Channel. *J Pharmacol Exp Ther* **301**:427-434.

Fernandez D, Ghanta A, Kauffman GW and Sanguinetti MC (2004) Physicochemical Features of the HERG Channel Drug Binding Site. *J Biol Chem* **279**:10120-10127.

Funck-Brentano C, Kroemer HK, Lee JT and Roden DM (1990) Propafenone. *N Engl J Med* **322**:518-525.

Gessner G, Zacharias M, Bechstet S, Schonherr R and Heinemann SH (2004) Molecular Determinants for High-Affinity Block of Human EAG Potassium Channels by Antiarrhythmic Agents. *Mol Pharmacol* **65**:1120-1129.

Hii JT, Wyse DG, Gillis AM, Cohen JM and Mitchell LB (1991) Propafenone-Induced Torsade De Pointes: Cross-Reactivity With Quinidine. *Pacing Clin Electrophysiol* **14**:1568-1570.

Ishii K, Kondo K, Takahashi M, Kimura M and Endoh M (2001) An Amino Acid Residue Whose Change by Mutation Affects Drug Binding to the HERG Channel. *FEBS Lett* **506**:191-195.

Jiang Y, Lee A, Chen J, Cadene M, Chait BT and Mackinnon R (2002) Crystal Structure and Mechanism of a Calcium-Gated Potassium Channel. *Nature* **417**:515-522.

Kamiya K, Mitcheson JS, Yasui K, Kodama I and Sanguinetti MC (2001) Open Channel Block of HERG K⁺ Channels by Vesnarinone. *Mol Pharmacol* **60**:244-253.

MOL # 1743

- Lees-Miller JP, Duan Y, Teng GQ and Duff HJ (2000) Molecular Determinant of High-Affinity Dofetilide Binding to HERG1 Expressed in *Xenopus* Oocytes: Involvement of S6 Sites. *Mol Pharmacol* **57**:367-374.
- Levi AJ, Hancox JC, Howarth FC, Croker J and Vinnicombe J (1996) A Method for Making Rapid Changes of Superfusate Whilst Maintaining Temperature at 37 Degrees C. *Pflügers Arch* **432**:930-937.
- McGaughey GB, Gagné M and Rappé AK (1998) Π -Stacking Interactions. Alive and Well in Proteins. *J Biol Chem* **273**:15458-15463.
- Mergenthaler J, Haverkamp W, Huttenhofer A, Skryabin BV, Musshoff U, Borggreffe M, Speckmann EJ, Breithardt G and Madeja M (2001) Blocking Effects of the Antiarrhythmic Drug Propafenone on the HERG Potassium Channel. *Naunyn Schmiedebergs Arch Pharmacol* **363**:472-480.
- Milnes JT, Crociani O, Arcangeli A, Hancox JC and Witchel HJ (2003) Blockade of HERG Potassium Currents by Fluvoxamine: Incomplete Attenuation by S6 Mutations at F656 or Y652. *Br J Pharmacol* **139**:887-898.
- Mitcheson JS, Chen J, Lin M, Culberson C and Sanguinetti MC (2000a) A Structural Basis for Drug-Induced Long QT Syndrome. *Proc Natl Acad Sci U S A* **97**:12329-12333.
- Mitcheson JS, Chen J and Sanguinetti MC (2000b) Trapping of a Methanesulfonanilide by Closure of the HERG Potassium Channel Activation Gate. *J Gen Physiol* **115**:229-240.
- Paul A, Witchel HJ and Hancox JC (2001) Inhibition of HERG Potassium Channel Current by the Class 1a Antiarrhythmic Agent Disopyramide. *Biochem Biophys Res Commun* **280**:1243-1250.

MOL # 1743

Paul AA, Witchel HJ and Hancox JC (2002) Inhibition of the Current of Heterologously Expressed HERG Potassium Channels by Flecainide and Comparison With Quinidine, Propafenone and Lignocaine. *Br J Pharmacol* **136**:717-729.

Perry M, De Groot MJ, Helliwell R, Leishman D, Tristani-Firouzi M, Sanguinetti MC and Mitcheson JS (2004) Structural Determinants of HERG Channel Block by Clofilium and Ibutilide. *Mol Pharmacol* **Epub ahead of print**:21 May 2004.

Rehnqvist N, Ericsson CG, Eriksson S, Olsson G and Svensson G (1984) Comparative Investigation of the Antiarrhythmic Effect of Propafenone (Rytmonorm) and Lidocaine in Patients With Ventricular Arrhythmias During Acute Myocardial Infarction. *Acta Med Scand* **216**:525-530.

Ridley JM, Milnes JT, Benest AV, Masters JD, Witchel HJ and Hancox JC (2003) Characterisation of Recombinant HERG K⁺ Channel Blockade by the Class Ia Antiarrhythmic Drug Procainamide. *Biochem Biophys Res Commun* **306**:388-393.

Roden DM, Lazzara R, Rosen M, Schwartz PJ, Towbin J and Vincent GM (1996) Multiple Mechanisms in the Long-QT Syndrome. Current Knowledge, Gaps, and Future Directions. The SADS Foundation Task Force on LQTS. *Circulation* **94**:1996-2012.

Sanchez-Chapula JA, Navarro-Polanco RA, Culberson C, Chen J and Sanguinetti MC (2002) Molecular Determinants of Voltage-Dependent Human Ether-a-Go-Go Related Gene (HERG) K⁺ Channel Block. *J Biol Chem* **277**:23587-23595.

Sanguinetti MC, Jiang C, Curran ME and Keating MT (1995) A Mechanistic Link Between an Inherited and an Acquired Cardiac Arrhythmia: HERG Encodes the I_{Kr} Potassium Channel. *Cell* **81**:299-307.

MOL # 1743

Sanguinetti MC and Xu QP (1999) Mutations of the S4-S5 Linker Alter Activation Properties of HERG Potassium Channels Expressed in *Xenopus* Oocytes. *J Physiol (Lond)* **514**:667-675.

Smart OS, Neduvilil JG, Wang X, Wallace BA and Sansom MS (1996) HOLE: a Program for the Analysis of the Pore Dimensions of Ion Channel Structural Models. *J Mol Graph* **14**:354-360.

Spector PS, Curran ME, Keating MT and Sanguinetti MC (1996) Class III Antiarrhythmic Drugs Block HERG, a Human Cardiac Delayed Rectifier K⁺ Channel. Open-Channel Block by Methanesulfonanilides. *Circ Res* **78**:499-503.

Footnotes

* This work was supported by project grant PG/2001104 from the British Heart Foundation and an MRC career establishment award (J.S.M.). Part of this work has been presented in abstract form in Witchel HJ, Perry M, Milnes JT, Hancox JC and Mitcheson JS (2003). Molecular determinants of HERG blockade by propafenone – drug trapping of a low potency voltage-dependent HERG blocker. *Biophys. J.* 84 (2 pt 2): 2660.

MOL # 1743

Figure Legends

Figure 1. Molecular determinants of blockade in the pore/S6 region.

A – J: representative current traces for HERG and mutant HERG channels in the absence (closed squares ■) and presence (open circles ○) of 50 μM propafenone. **A** shows the command voltage protocol for **B & C**, **D** shows the command protocol for **E - J**. **H & J** are the same as **E & F**, but with a close-up of the relevant time period. Ordinates are membrane current (I_{memb}) in μA . **K** shows the concentration-response curve for wild-type HERG peak tail currents in 2 mM K^+ . **L** shows a summary of mean current remaining with 50 μM propafenone in all mutants tested. $N = 3-5$ for all.

Figure 2. Rapid onset and reversibility of block by propafenone

This figure shows the first second of representative current traces elicited by a depolarising command protocol (depolarising step to 0 mV for 5 seconds, followed by a repolarising step to -120 mV for 1 second, interpulse interval 10 seconds) before drug addition, after 3 μM propafenone addition, and after washout of propafenone. After a steady HERG current baseline was established in control solution (“control”), propafenone-containing superfusate was washed on for two minutes to allow for complete fluid exchange while the oocyte remained at the holding potential (-90 mV). After four sweeps in propafenone (the first two of which are shown, PROPAF sweep # 1 and PROPAF sweep # 2), control superfusate was washed into the bath for five minutes while the voltage remained at the holding potential, and then the voltage command protocol was employed to elicit a final current (“washout”). Although the latter 700 ms of PROPAF sweeps # 1 and # 2 nearly overlay, the initial 100 ms of PROPAF sweep # 1 is nearly identical to the control trace, whereas the initial 100 ms of PROPAF sweep # 2 is nearly overlays the washout sweep # 1 trace. Capacitative transients are blanked. Typical of five cells.

MOL # 1743

Figure 3. Trapping and release of propafenone in D540K

To determine whether propafenone was trapped in the D540K channel, a protocol as in panel **A** (inset) was applied to the oocyte in the presence and absence of 3 μ M propafenone. Two other similar protocols (differing only in the final repolarising voltage) were also performed with the same cells. Panel **A** shows segment (see dotted box in inset for the segment shown) of a representative pair of D540K current traces that are attenuated in the presence of propafenone during depolarisation, but during repolarisation to -120 mV drug blockade is eliminated. The diamonds represent three of the four time points (left to right: end pulse, peak tail, 200 ms) at which analysis of mean currents were performed. **B** shows the mean D540K block at different times during protocol in 2A.

Figure 4. Trapping of propafenone in wild-type HERG

The percentage blockade by 3 μ M propafenone of wild-type HERG current was not reduced by the duration of repolarisation at -120 mV. Potential was held at -90 mV, depolarised to 0 mV for 5 seconds, repolarised to -120 mV for increasing durations of time (20 ms to 120 ms in 20 ms steps), prior to depolarisation to 0 mV (three pulse protocol). Similar experiments were performed using voltages of -70 and -40 mV. **A** shows a representative series of traces for -120 mV deactivation steps, showing only the sweeps for time points at 40 ms and 120 ms for clarity (C = control, P = 3 μ M propafenone). In **B** the percentage block was calculated for each duration of repolarisation. N = 5 for all.

Figure 5. Reversibility of block while the channels are closed

The reversibility of wild-type HERG blockade was compared in the same oocytes after a 5 minute period of washout and after a 30 second period of washout; representative traces all from the same oocyte are shown in panels Ai & B. As functional blockade cannot be measured electrophysiologically except while open, a blockade “sampling protocol” was

MOL # 1743

employed (panel Aii) in which the membranes were strongly depolarised but for a minimal time (40 ms) in order to maximise tail currents while minimising time in the open-state when propafenone could exit from a trapped condition. To maintain a definitive closed state, all experiments in Figure 5 involved a holding potential of -120 mV; blockade was determined for the peak of the tail current elicited at -60 mV. Initially the oocytes were tested with the sampling protocol while superfused with control superfusate (control, panel Ai), and then were superfused with 10 μ M propafenone for one minute while held at -120 mV. Pseudo-steady-state blockade was elicited by depolarising the membrane to 0 mV for 2 seconds followed by 2 seconds at -70 mV (i.e. a single sweep similar to Figure 1A), and then blockade was measured using the sampling protocol (panel Ai, Propafenone, only two sweeps were allowed). Then, while the cell membrane potential was held at -120 mV, washout of propafenone was effected by superfusion of control solution for 5 minutes. The sampling protocol was applied again; the amount of block was calculated isochronally with the peak of the control current sweep. While superfusing control solution, the sampling protocol was applied repeatedly for 5 minutes (start-to-start interval = 10 seconds), which was sufficient for a steady-state baseline to be re-established (panel B, final sweep previous washout). The pseudo-steady-state blockade by propafenone (panel B, propafenone) followed by washout was repeated as above, except that washout was allowed to proceed for only 30 seconds at -120 mV before applying the sampling protocol (panel B, washout 30 seconds first sweep). Panel C shows the data for wild-type HERG, demonstrating that the percentage blockade is the same with each application of drug, and that recovery from block is identical after 5 minutes or 30 seconds of washout (e.g. panel Ai vs. panel B). Paired symbols connected by a line represent an individual oocyte. N = 3 oocytes. A similar series of experiments was performed for wild-type (WT) and a selection of mutant channels for the 5 minute washout period (panel D). F656A tail currents were measured at -140 mV, and the short

MOL # 1743

depolarisation to + 40 mV was slightly longer (60 ms) in duration for S624A to compensate for slower activation kinetics. The concentration of propafenone used for each mutant was chosen to elicit a fractional blockade of ~50% (wild-type 10 μ M, F656A 300 μ M, Y652A 30 μ M, V625A 30 μ M, and S624A 10 μ M). N = 3-6 for all.

Figure 6. Sequence homologies used in constructing HERG closed and open-state homology models

Sequences are annotated according to the location in the structural element of the channel. The top two lines are the sequences of HERG built onto the closed-state channel structure of KcsA (according to the homology with the KcsA sequence in line 3) and onto the open-state channel structure of MthK (according to the homology with the MthK sequence in line 4). Small numbers above the HERG sequences are the sequence numbers of KcsA or MthK that become transferred onto the HERG homology models. The HERG amino acid sequence numbers are shown in larger font below the HERG/KcsA alignment (*i.e.* Y652 of HERG aligns with F103 of KcsA and F87 of MthK).

Figure 7. Modelled docking of propafenone

Lowest score structures of propafenone docked into closed (**A**) and open-state (**B**) homology models (extracellular surface at top); panels **C** and **D** are stereo views of the propafenone binding-site in closed- and open-state models, respectively. Y652 (red) and F656 (yellow) side-chains are displayed along with backbone ribbons (grey). Propafenone carbons are coloured green. Panels E and F show line diagrams of the atomic coordinates of the closed (left) and open (right) HERG homology models, with the accessible channel pore regions, determined using HOLE (Smart *et al.*, 1996), stippled green. The side-chains of Y652 (red) and F656 (yellow) are shown with solid rendering. Note that in the closed-channel model the inner cavity is constricted at the level of F656, and as such would prevent

MOL # 1743

simultaneous π stacking interactions between propafenone's two aromatic rings and two of the F656 residues.

Figure 8. Aromatic ring interactions between the drug and HERG models.

Propafenone docking to open-state (open circles) and closed-state (filled circles) HERG homology models was characterised in terms of aromatic ring (π : π) interactions. Each docking run was ranked by energy (see key in bottom panel), and defined by the number of HERG Y652 or F656 aromatic ring atoms within 4.5 angstroms of a propafenone aromatic ring atom. A distance cutoff of 4.5 angstroms was taken to be the maximum separation of aromatic ring atoms that give rise to energetically favourable π -stacking interactions (McGaughey *et al.*, 1998; Chelli *et al.*, 2002). The maximum number of ring atoms per Y652 or F656 was taken to be 11 (all ring carbons and ring bound atoms *ortho*, *meta* or *para* to the carbon atom linking the ring to the β carbon of the side-chain). Thus, a docking run in which all 4 Y652's (or F656's) made maximum interactions with propafenone aromatic rings would have a value of 44, and a value of 10-11 corresponds to approximately 1 (parallel) π -stacking interaction between propafenone and the HERG model. Outliers in the closed-state model represent conformations in which the binding-site was constrained to be F656, S660 and all atoms within 4.5 Å (i.e. excluding Y652), and in these cases FlexiDock could not locate a low energy binding state. A few low energy open-state docking results were found with significant Y652 interactions (outliers in the top left corner of the figure) but these conformers also made significant additional contacts with F656. The large majority of runs with the open channel found low energy binding states exhibiting a large number of propafenone interactions with F656, and these were the only set of binding modes in either open or closed-channel models that were consistent with the mutagenesis data described above.

MOL # 1743

Figure 9. Structural formulae of propafenone, MK-499, and clofilium

MOL # 1743

Tables

Table 1: FlexiDock analysis of drug binding to HERG homology models

drug	channel state^a	lowest energy score	# of runs	# of generations
Propaf	closed	-192	33	3,940,000
"	open	-207	27	4,210,000
MK-499	closed	-137	26	3,716,000
"	open	-198	11	1,140,000

Table 1. FlexiDock analysis of drug binding to HERG homology models

^a Binding-site normally defined as G648/S649/Y652/F656/S660 and all atoms within 4.5 Å.

All side-chain bonds in binding-site were allowed to rotate.

MOL # 1743

Table 2

Channel	Voltage step	K⁺	IC₅₀ μM	95% CI IC₅₀	n_{Hill}	95% CI n_{Hill}
Wild Type	-70 mV	2 mM	2.16	1.98 to 2.34	1.09	0.99 to 1.20
Wild Type	-70 mV	96 mM	4.38	3.76 to 5.11	0.94	0.81 to 1.07
F656A	-140 mV	2 mM	205	83 to 506	1.86	-0.99 to 4.71
Y652A	-70 mV	2 mM	13.6	8.2 to 22.4	1.25	0.49 to 2.00
V625A	-70 mV	2 mM	12.1	6.8 to 21.5	0.63	0.32 to 0.94

Table 2. Summary concentration response data

Summary of the concentration response data from wild-type HERG, F656A, Y652A and V625A tail currents under the conditions listed. The fit of F656A block by propafenone resulted in an abnormally large Hill Slope (n_{Hill}), probably due to fitting of only three points of the curve; higher concentrations were associated with solubility issues as explained in the text. By fixing the Hill slope to 1, the IC₅₀ was found to be 246 μM. The Hill slope of V625A may be slightly less than one due to effects of this mutation on the selectivity of the channel. CI = confidence interval.

Figure 1

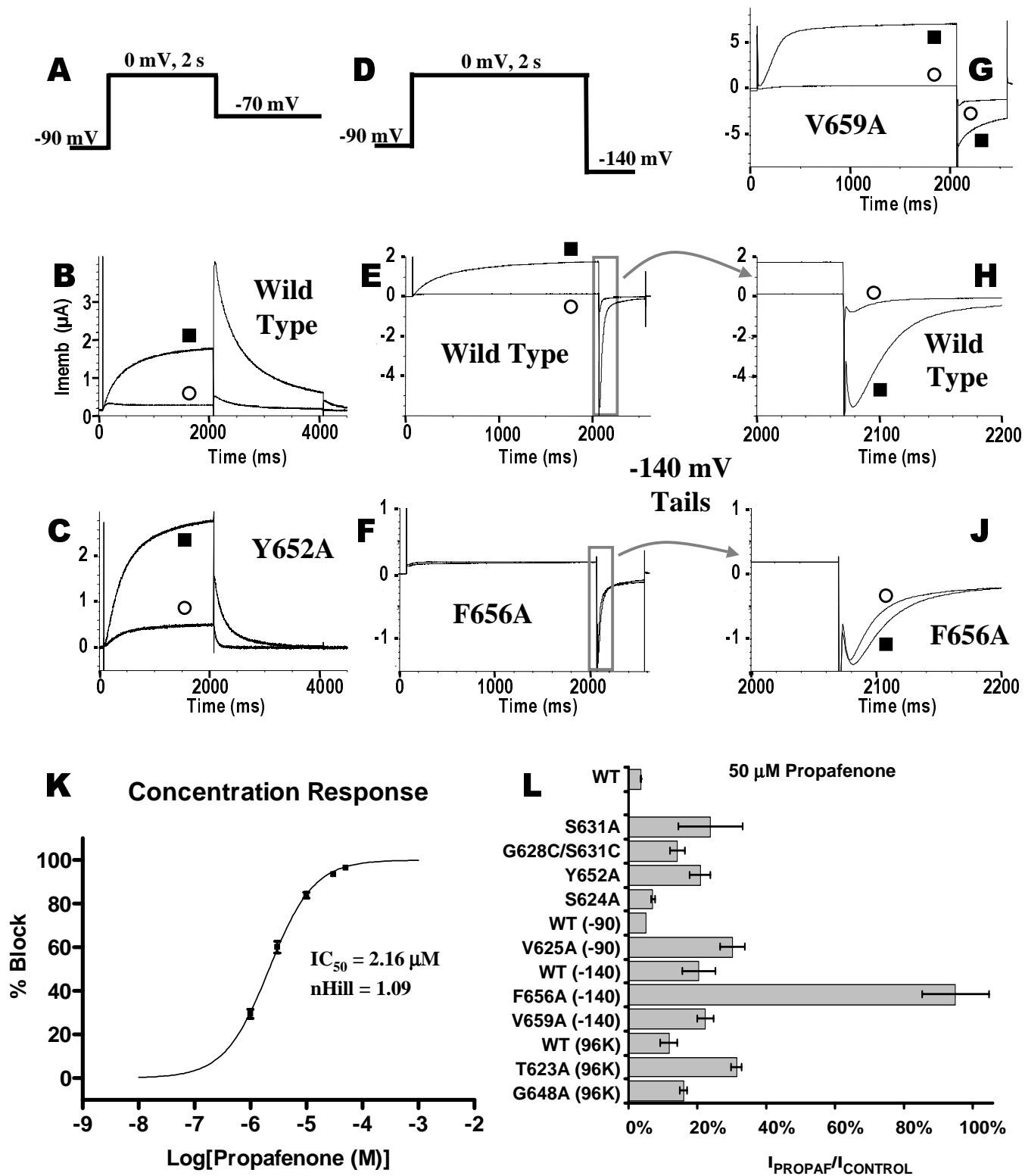
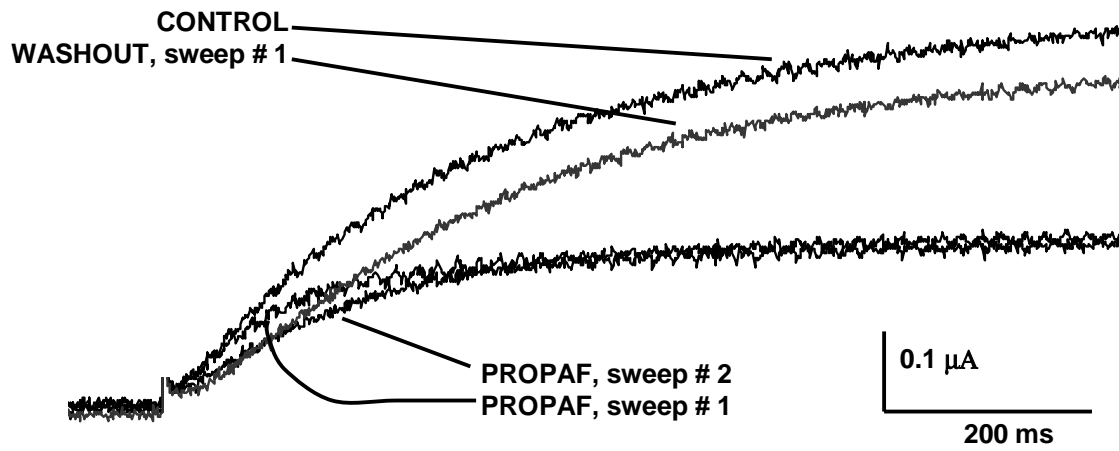


Figure 2



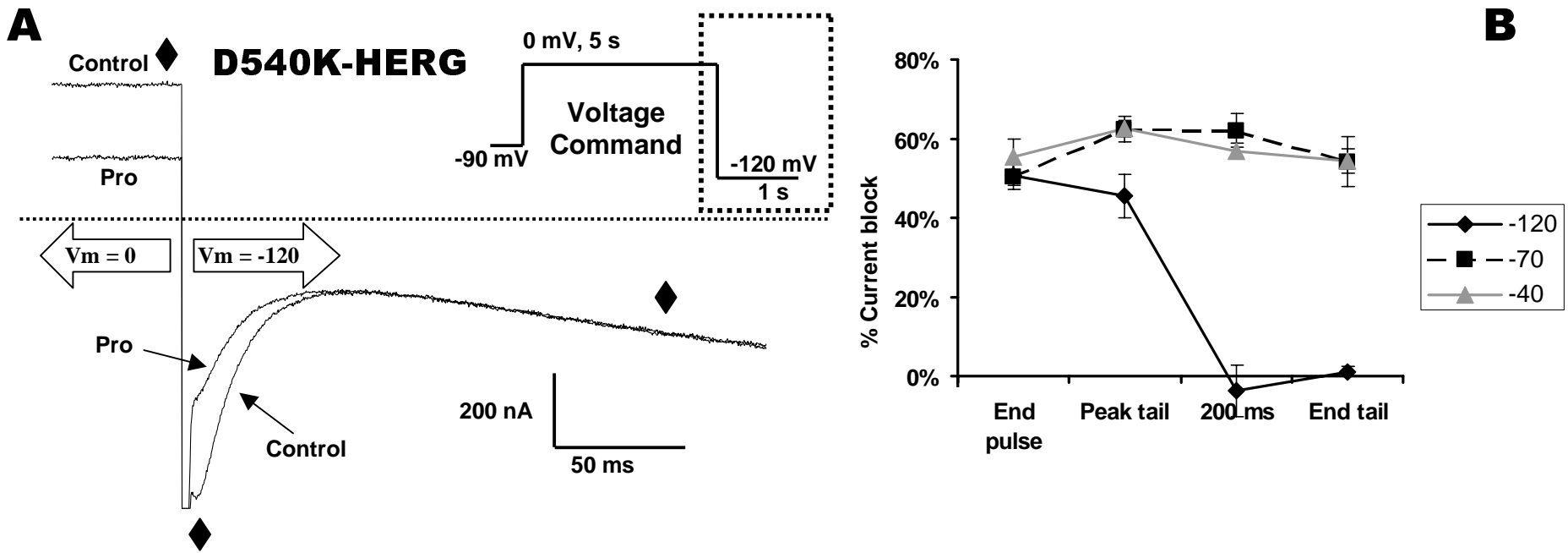


Figure 3

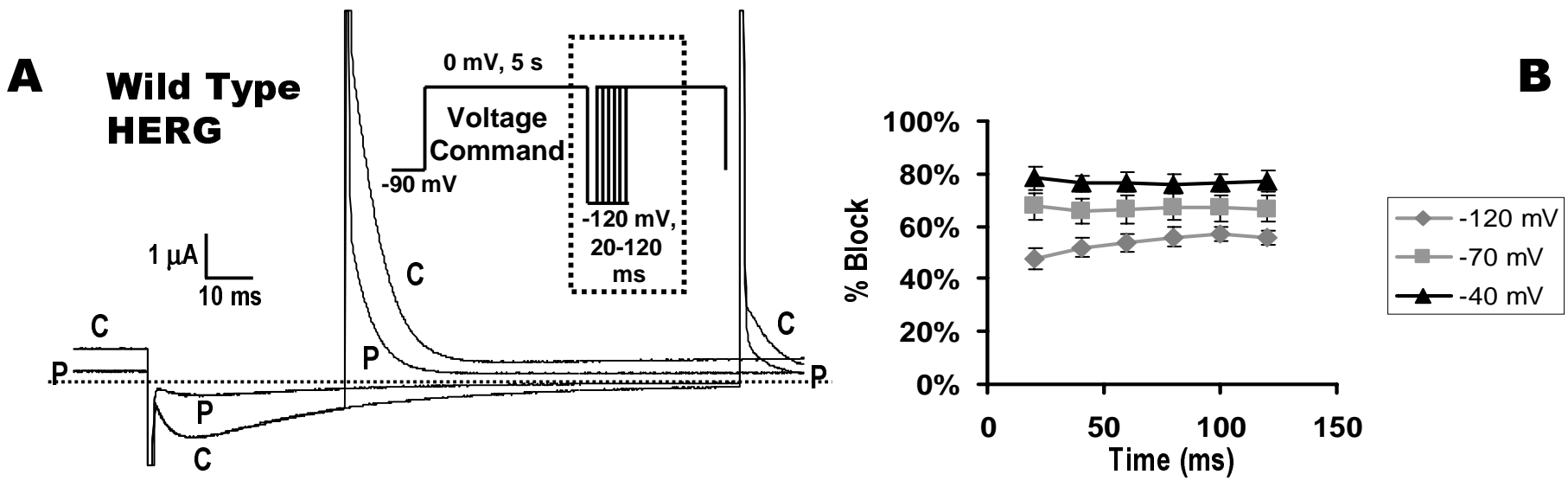


Figure 4

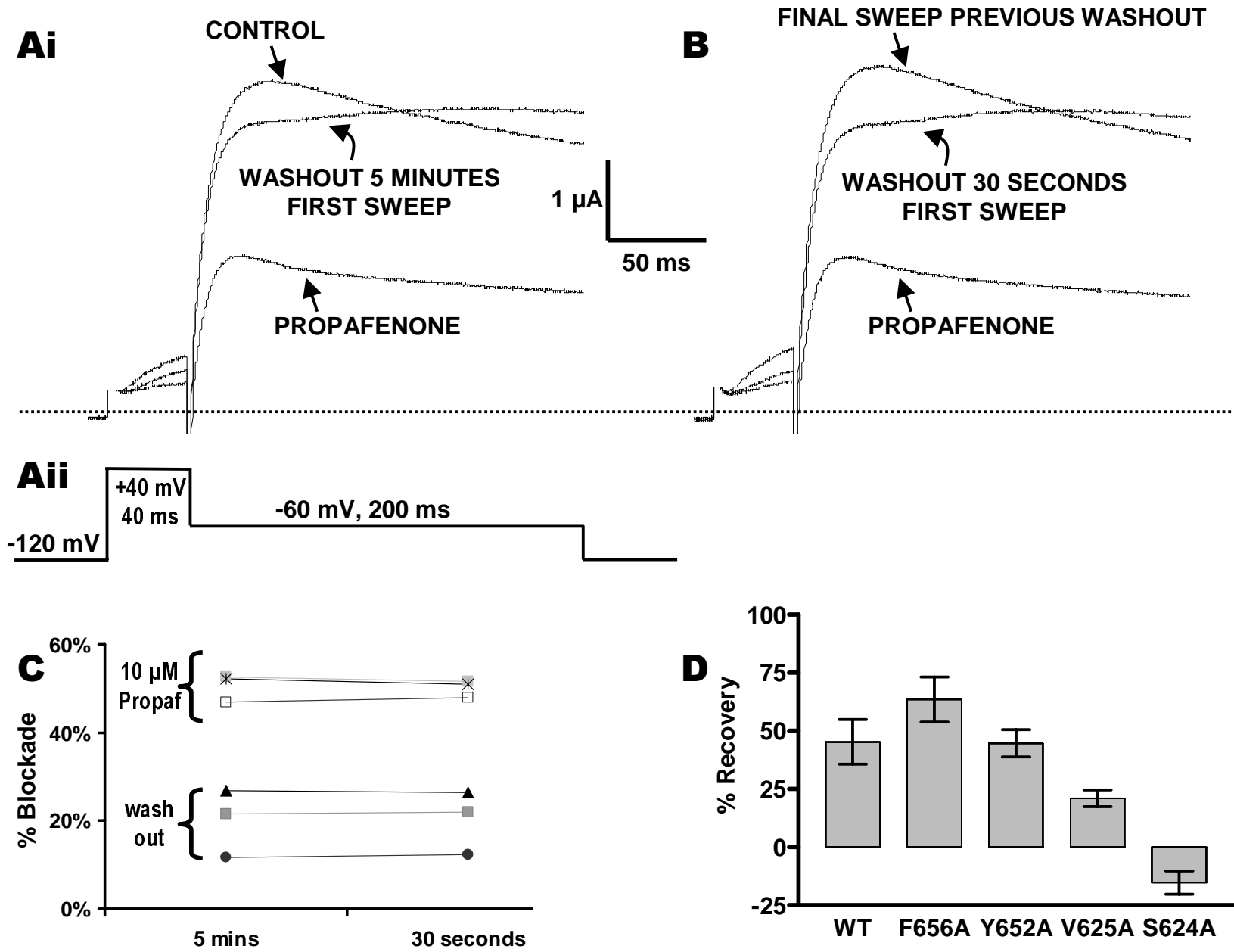


Figure 5

Figure 6

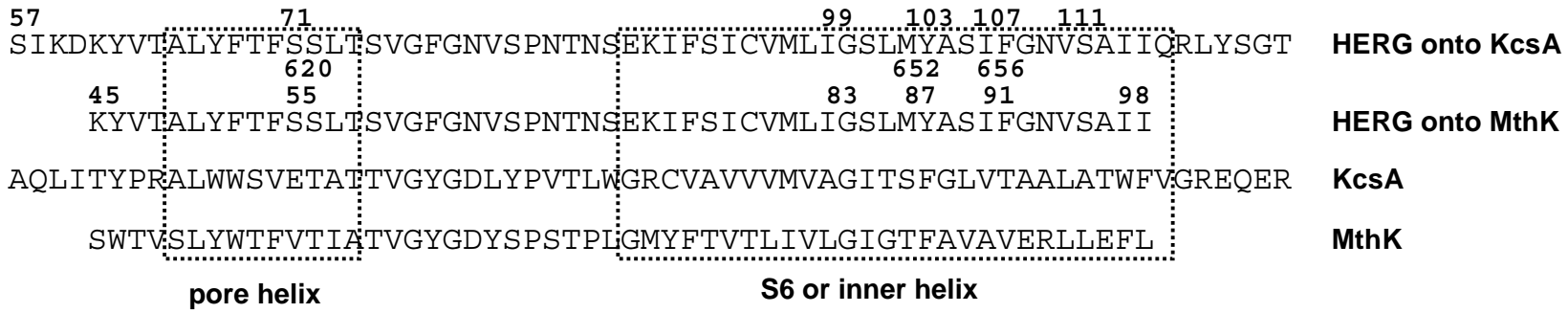


Figure 7

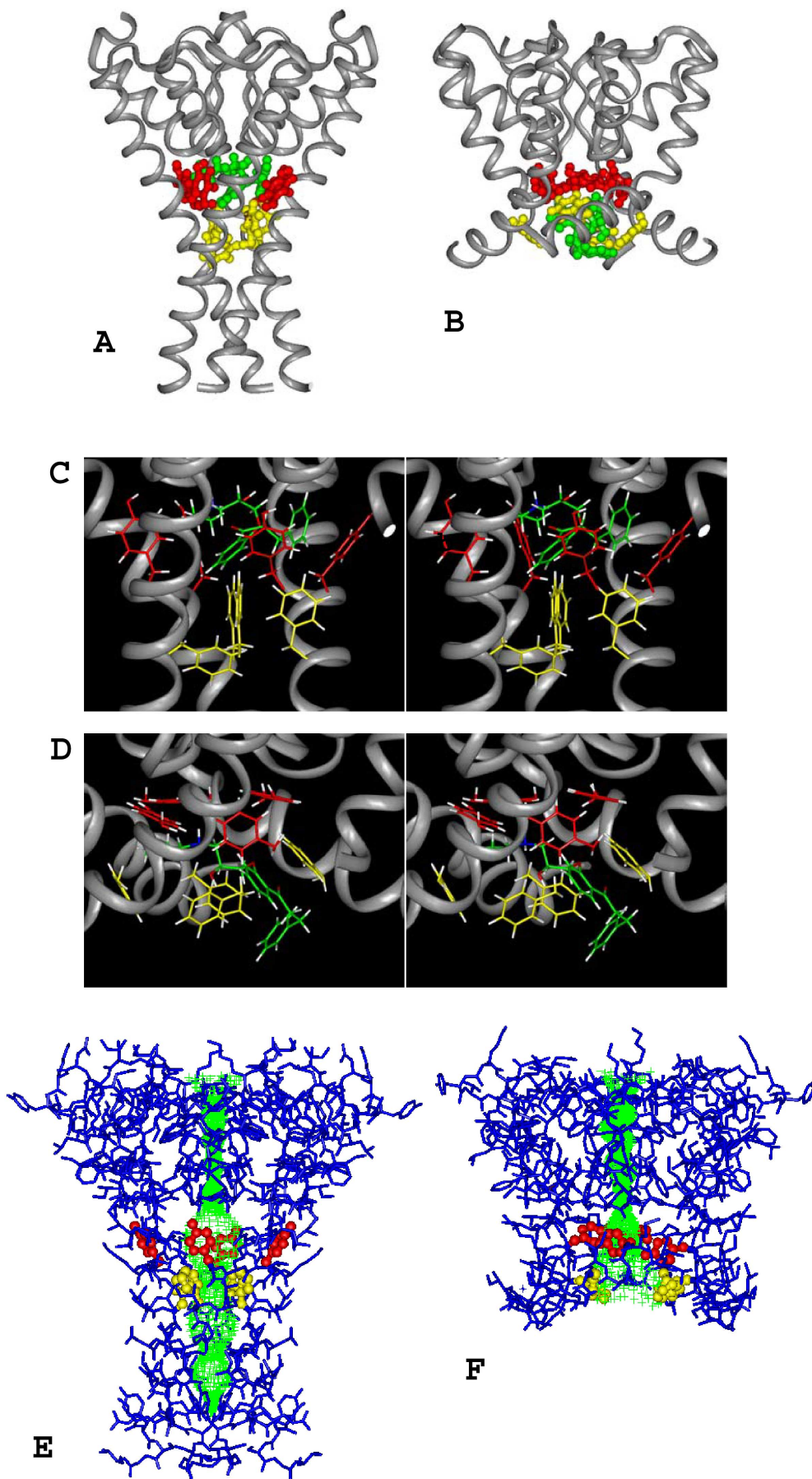
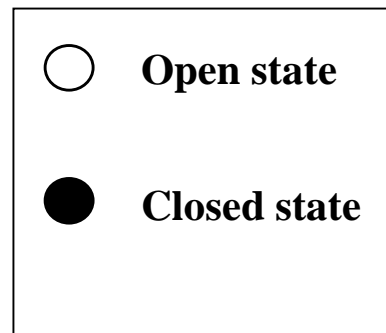
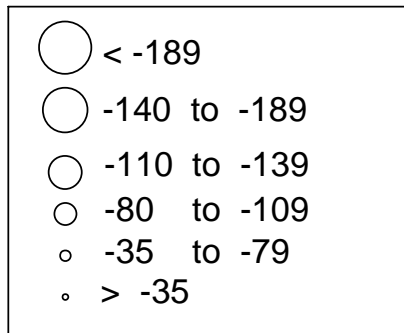
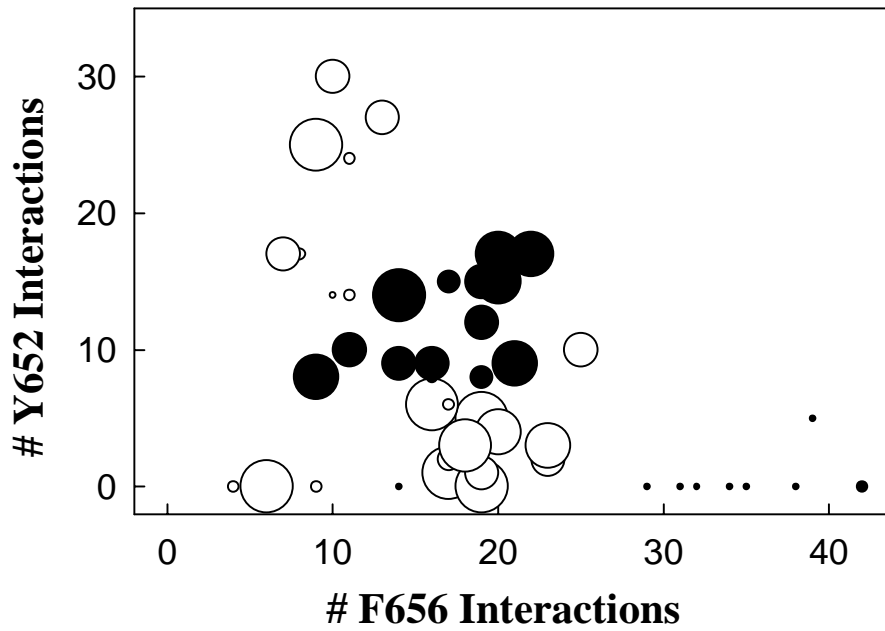


Figure 8



Flexidock "energy" scores

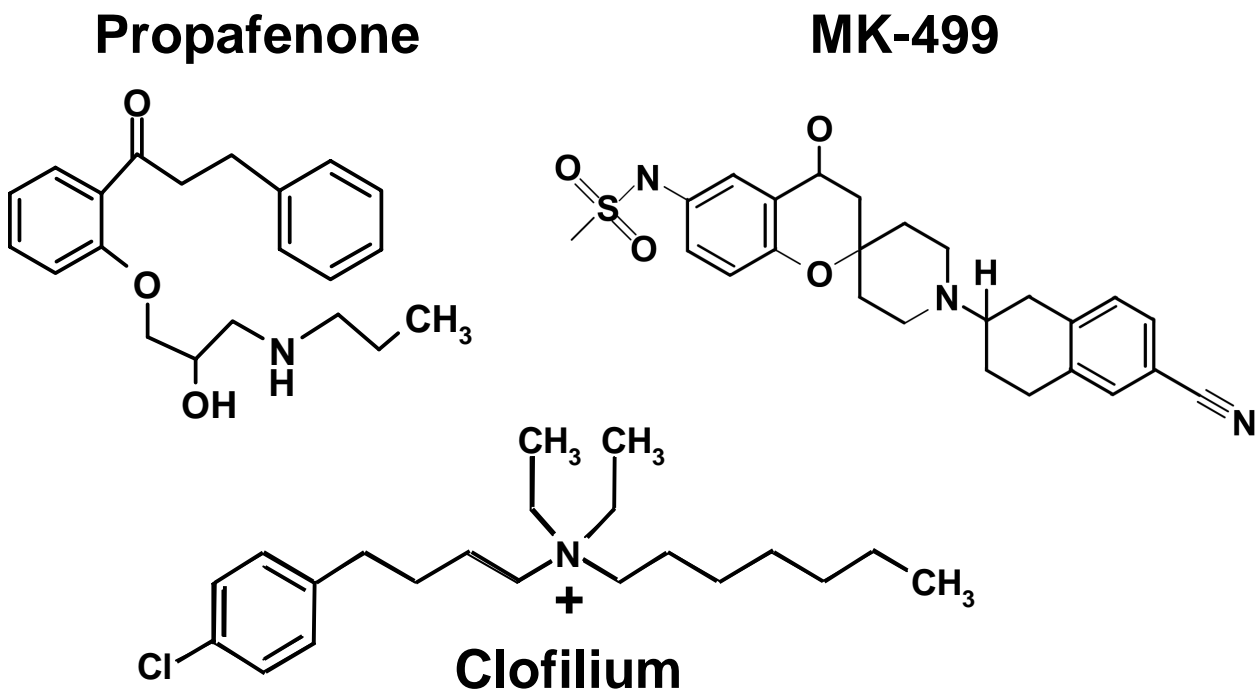


Figure 9